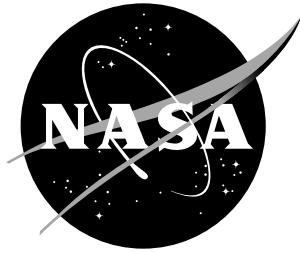NASA/CR-97-206263

Honeycomb Core Permeability Under Mechanical Loads

David E. Glass, V. V. Raman, Venki S. Venkat, and Sankara N. Sankaran
Analytical Services and Materials, Inc., Hampton, VA

December 1997

The NASA STI Program Office ... in Profile

Since its founding, NASA has been dedicated to the advancement of aeronautics and space science. The NASA Scientific and Technical Information (STI) Program Office plays a key part in helping NASA maintain this important role.

The NASA STI Program Office is operated by Langley Research Center, the lead center for NASA's scientific and technical information. The NASA STI Program Office provides access to the NASA STI Database, the largest collection of aeronautical and space science STI in the world. The Program Office is also NASA's institutional mechanism for disseminating the results of its research and development activities. These results are published by NASA in the NASA STI Report Series, which includes the following report types:

- TECHNICAL PUBLICATION. Reports of completed research or a major significant phase of research that present the results of NASA programs and include extensive data or theoretical analysis. Includes compilations of significant scientific and technical data and information deemed to be of continuing reference value. NASA counter-part of peer reviewed formal professional papers, but having less stringent limitations on manuscript length and extent of graphic presentations.

- TECHNICAL MEMORANDUM. Scientific and technical findings that are preliminary or of specialized interest, e.g., quick release reports, working papers, and bibliographies that contain minimal annotation. Does not contain extensive analysis.

- CONTRACTOR REPORT. Scientific and technical findings by NASA-sponsored contractors and grantees.

- CONFERENCE PUBLICATION. Collected papers from scientific and technical conferences, symposia, seminars, or other meetings sponsored or co-sponsored by NASA.

- SPECIAL PUBLICATION. Scientific, technical, or historical information from NASA programs, projects, and missions, often concerned with subjects having substantial public interest.

- TECHNICAL TRANSLATION. English-language translations of foreign scientific and technical material pertinent to NASA's mission.

Specialized services that help round out the STI Program Office's diverse offerings include creating custom thesauri, building customized databases, organizing and publishing research results ... even providing videos.

For more information about the NASA STI Program Office, you can:

- Access the NASA STI Program Home Page at http://www.sti.nasa.gov/STI-homepage.html

- E-mail your question via the Internet to help@sti.nasa.gov

- Fax your question to the NASA Access Help Desk at (301) 621-0134

- Phone the NASA Access Help Desk at (301) 621-0390

- Write to:
  NASA Access Help Desk
  NASA Center for AeroSpace Information
  800 Elkridge Landing Road
  Linthicum Heights, MD 21090-2934

NASA/CR-97-206263
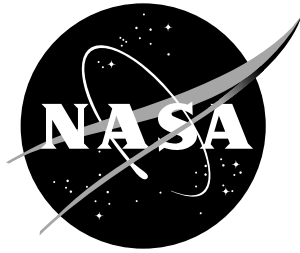
Honeycomb Core Permeability Under Mechanical Loads

David E. Glass, V. V. Raman, Venki S. Venkat, and Sankara N. Sankaran
Analytical Services and Materials, Inc., Hampton, VA

December 1997

The use of trademarks or names of manufacturers in this report is for accurate reporting and does not constitute an official endorsement, either expressed or implied, of such products or manufacturers by the National Aeronautics and Space Adminstration or by Analytical Services & Materials, Inc.

Honeycomb Core Permeability Under Mechanical Loads

David E. Glass, V. V. Raman, Venki S. Venkat, and Sankara N. Sankaran

Analytical Services & Materials, Inc.
107 Research Drive
Hampton, VA 23666

Abstract

A method for characterizing the air permeability of sandwich core materials as a function of applied shear stress was developed. The core material for the test specimens was either Hexcel HRP-3/16-8.0 or DuPont Korex-1/8-4.5 and was nominally one-half inch thick and six inches square. The facesheets where made of Hercules' AS4/8552 graphite/epoxy (Gr/Ep) composites and were nominally 0.059-in. thick. Cytec's Metalbond 1515-3M epoxy film adhesive was used for co-curing the facesheets to the core. The permeability of the specimens during both static (tension) and dynamic (reversed and non-reversed) shear loads were measured. The permeability was measured as the rate of air flow through the core from a circular 1-in^2 area of the core exposed to an air pressure of 10.0 psig. In both the static and dynamic testing, the Korex core experienced sudden increases in core permeability corresponding to a core catastrophic failure, while the HRP core experienced a gradual increase in the permeability prior to the core failure. The Korex core failed at lower loads than the HRP core both in the transverse and ribbon directions.

Introduction

Fibrous composite materials are being considered for commercial aircraft fuselage structures due to potential reductions in acquisition cost and weight. Composite sandwich structures are being developed for the keel and side panel, and may be adopted for the crown panel of a commercial fuselage [1-2]. A critical issue for the sandwich concept is environmental durability. Fuselage skin panels will be exposed to water from both the interior and exterior of the airplane in service. Other fluids, such as solvents and hydraulic fluids, will also be encountered, though less frequently and only in local areas. Exposure to these fluids in combination with thermal and mechanical loads can result in degradation of some composite structures. Sandwich structures have been observed to absorb moisture to the point of saturation, resulting in weight gain, degradation of core and facesheet materials, and degradation of the core-to-facesheet bond. In addition, poor quality repairs of damaged sandwich structures may result. It is thus important to understand the fluid ingression paths in composite structures as well as the fluid effects on the structure.

A majority of work performed on the effects of fluids on composites is related to moisture diffusion in composite laminates and the associated effects on material properties. Both Fickian and non-Fickian moisture diffusion have been observed in carbon/epoxy composites [3-6]. The rate of diffusion is primarily dependent on temperature but is also influenced by moisture concentration or stress. Non-Fickian diffusion has been observed at room temperatures and generally is accompanied by matrix swelling and void formation, while Fickian diffusion was observed at elevated temperatures. Absorbed water has been found to suppress the glass transition temperature of the matrix resin, thus degrading the elevated temperature performance [4]. It has also been determined that absorbed water may plasticize the resin matrix and degrade the fiber/matrix bond [5]. Moisture sorption may reduce resistance to transverse matrix cracking caused by thermal and/or mechanical loads [7]. Stress relaxation in the matrix resin at elevated temperature with absorbed water has been shown to alter the static mechanical strain required to initiate matrix cracking. Severe matrix cracking in sandwich facesheets may provide a path for liquid ingression into the core.

The effects of freeze-thaw cycling on water ingression in sandwich structures have been evaluated [8]. Both damaged and undamaged carbon/epoxy sandwich panels with glass/phenolic and Nomex honeycomb core materials were subjected to freeze-thaw cycling in a humid atmosphere. The undamaged panels exhibited no water ingression after 1000 cycles, while water ingression was observed in damaged panels with glass/phenolic core but not with the Nomex core. Several damaged carbon/epoxy and glass epoxy sandwich panels with Nomex core were evaluated by exposure to freeze/thaw cycling with humidity at Boeing. All the panels absorbed moisture but only one panel showed liquid water in the core [9]. In other tests at Boeing, water ingression occurred in carbon/epoxy sandwich panels with Nomex core wherever the finish or barrier film was damaged.

A test method for detecting fluid ingression paths in sandwich panels by measuring air permeability of the facesheet was developed at Boeing [9]. The facesheet permeability test method was extended to the evaluation of impact damage in sandwich structures. Boeing has also conducted permeability tests on coupons cut from specimens that had been loaded in three point flexure. The tests, however, were not conducted while the specimen was loaded. The Boeing tests demonstrated that Hexcel HRP honeycomb core material exhibited resistance to damage at shear stress levels up to 60% of the ultimate strength in the ribbon direction, and up to 70% in the transverse direction. DuPont Korex honeycomb core material exhibited resistance to damage at shear stress levels up to 75% of the ultimate strength in the ribbon direction, and up to 90% in the transverse direction. The air permeability in the HRP core material gradually increased with stress once damage appeared. In the Korex material transverse direction, the permeability increased from 0.0 ml/min/psi to 14.46 ml/min/psi with an increase in the shear stress of only 12 psi. In the ribbon direction, the Korex material did not see significant increases in the permeability at the tested shear stress levels.

The environmental durability of the sandwich panels must be demonstrated prior to use in fuselage skin panels. The resistance of the core material to damage that would allow internal migration of fluids from local ingression points must also be understood. Characterizing the air permeability of sandwich core materials as a function of applied transverse shear stress is an important step in understanding the usefulness of the sandwich panels. The air permeability, defined as the flow rate (ml/min) divided by applied pressure (psi), will give an indication of how fluids migrate in the structure. The objective of this work was to determine how the air permeability in honeycomb sandwich specimens increased as a function of applied shear stress. An existing test machine was used along with a method developed to apply 10 psig air to the internal honeycomb core.

The HRP and Korex honeycomb cores were evaluated under both static and dynamic (reversed and non-reversed) loads.

Experimental Approach

To determine the permeability of the honeycomb core sandwich panels under shear loads, an apparatus was constructed that enabled both static and dynamic loads to be applied while the honeycomb core was exposed to a constant 10 psig air supply. A data acquisition system was assembled to monitor and acquire the test data. A discussion of the apparatus, the data acquisition system, and the specimen fabrication follows.

Apparatus

The maximum load required in the samples was estimated to be 27,000 lb, based on shear strength of the honeycomb core reported by the manufacturer. AS&M used an existing servohydraulic universal testing machine (UTM) to apply the desired load. The loading scheme was in conformance with ASTM C273-61 (reapproved in 1988). The test fixture used initially was designed and fabricated by Wyoming Test Fixtures. The test fixture was used successfully for all the static tests and kept the samples properly aligned for each test.

When the test fixture was used for the non-reversed load fatigue tests, the component of the fixture which is bolted to the loading plate cracked. A replacement for this part was procured from Wyoming Test Fixtures, which also cracked. A further replacement of this part was made after an in-house modification of its design, consisting of increased moment of inertia, higher fillet radii, and choice of a different grade of steel. After replacement, all the non-reversed load fatigue tests were carried out successfully.

However, when reversed loading was attempted using the above fixtures, extensive relative displacement of the loading plate with the fixture was noticed. This was because the clamping based on friction would work only if the tension in each bolt was on the order of the applied tension on the specimen assembly. This is unlike the situation during non-reversed loading when one-time displacement and bolt-to-hole contact would eliminate the need for frictional support. Attempts to increase bolt tension resulted in the failure of the bolts. In order to overcome this, a new design, based on direct support on the bolts rather than friction, was made. For this purpose, the bolt holes and bolts were made conical and the nuts were tightened over washers. Figure 1 shows a schematic diagram of the redesigned bolt used for the testing. The redesign ensured 360° contact between the holes and the bolts, eliminating any scope for relative displacement during loading. With this modification, all the reversed load fatigue tests were carried out successfully.

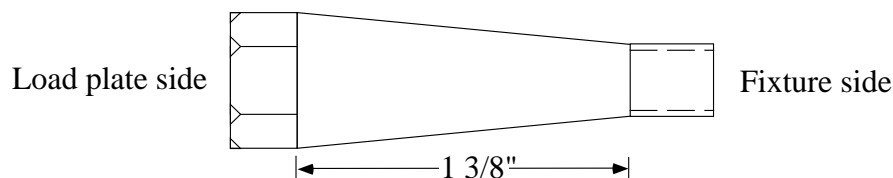Load plate side   Fixture side

|← 1 3/8" →|

Figure 1:   Schematic diagram of the redesigned, tapered bolt used for the fully reversed tests.

A load plate is shown in Figure 2 attached to the fixture which connects the load plate to the load cell. Four tapered holes in the flange region of the load plate were used for the connection. Both the holes in the load plate and the holes in the fixture were tapered for the tapered bolts shown above.
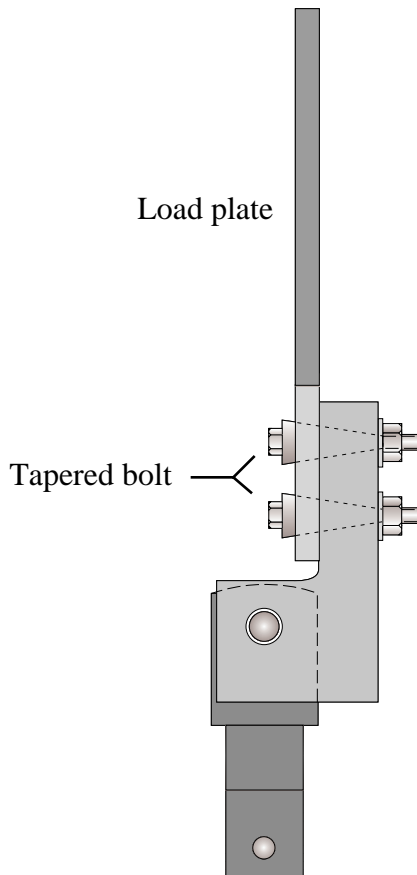
Load plate

Tapered bolt

Figure 2: Schematic diagram of the fixture connected to the load plate with the tapered bolts.

Data Acquisition

Personal computers (PC's) were used to acquire the data. The electrical output signals from the load-cell conditioner of the UTM, the mass flow meter, and the capacitance manometer were input to the computers through appropriate interface units, as shown in Figure 3.

Data acquisition during the tests was carried out by an IBM-compatible PC through a Hewlett Packard 3497A data acquisition unit. During the static tests, the signals monitored were from the load cell conditioner of the UTM, the capacitance manometer, and the mass flow meter, all as a function of time. The signals were stored in the hard disk at uniform intervals of time.

During fatigue testing, the test was controlled at a pre-determined mean and amplitude of the pulsating load which was displayed in the display unit of the machine. The only parameters monitored by the computer were the pressure and flow rate, which were generated by the respective transducers mentioned above. Data was recorded both at timed intervals and also when the signals underwent significant changes in their values.

Timed intervals were incremented in such a way that while finer resolution was available during the initial cycles, a larger number of cycles could be accommodated in a data set of reasonable size. This did not come in the way of detecting failure, as such events would cause recording of data irrespective of the time interval.
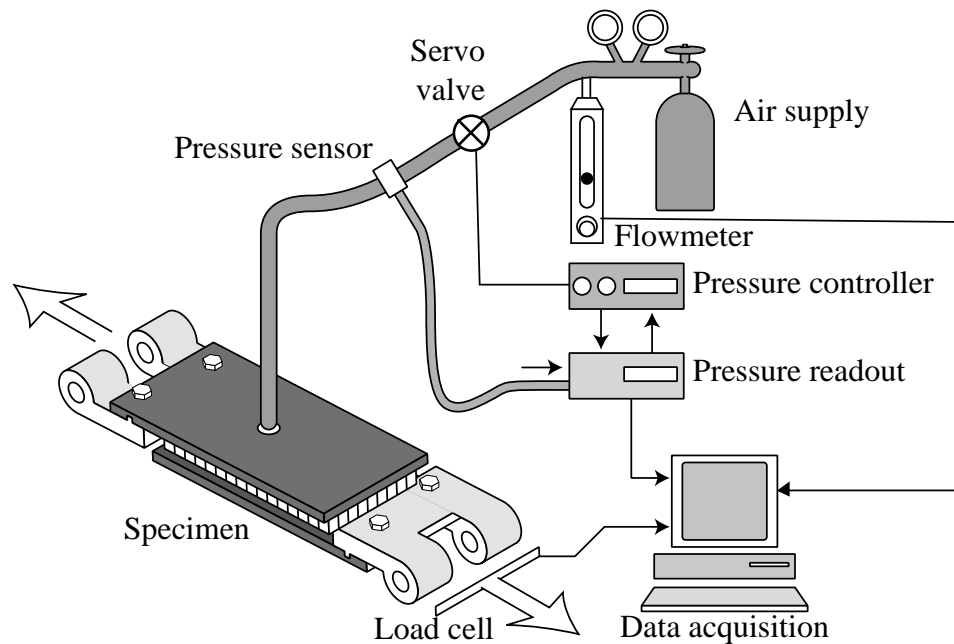

Figure 3: Schematic diagram of test set-up for permeability shear tests.

The 10.0 psig air supply was produced from a bottle of high pressure air. A pressure controller was used to control the air pressure. The pressure was monitored through a capacitance manometer. A flow meter was used to determine the flowrate of the air to an accuracy of 1 ml/min. The air flow rate was measured between the air supply and the pressure controller, as shown in Figure 3.

Specimens

Boeing supplied AS&M with two sandwich core panels. One panel had a dimension of 36 in. x 36 in., and contained Hexcel HRP-3/16-8.0 honeycomb core. The other panel had a dimension of 44 in. x 26 in. and contained DuPont Korex-1/8-4.5 honeycomb core. The facesheets where made of Hercules' AS4/8552 graphite/epoxy (Gr/Ep) composites and were nominally 0.059-in. thick. Cytec's Metalbond 1515-3M epoxy film adhesive was used for co-curing the facesheets to the core. In both cases, the core thickness was nominally 0.5 in. and the total sandwich panel thickness was nominally 0.62 in. Specimens with a dimension of 6 in. x 6 in. were cut from each panel. The edges of the panel were not included in the specimen area in order to eliminate the inclusion of any edge effects that may have occurred during the co-cure fabrication. After the specimens were cut, 14 holes with a 3/16 in. diameter were drilled through one facesheet in a 1 in. diameter area in the center of the facesheet. The photograph in Figure 4 shows the 14 holes in the center of a 6 in. x 6 in. specimen. Care was taken to minimize damage to the honeycomb core during the drilling of the holes. Also shown in Figure 4 is a load plate with a 1 in^2 circular area counter-sunk bore that matched the location of the holes in the specimen. On the opposite side of counter-sunk bore is a 0.25

in. threaded hole for the air supply. Also seen in Figure 4 is the fixture used to align the load plates when bonding.
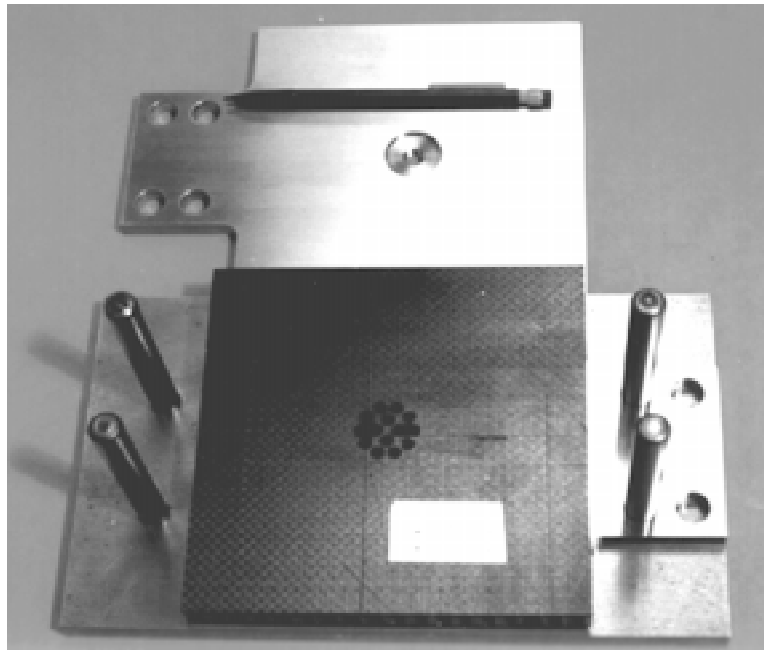

Figure 4:   Photograph of a load plate, specimen, and bonding fixture.

The precipitation hardened stainless steel load plates were bonded to the outside of each facesheet with Hysol EA 9309NA room temperature cure adhesive. Initially, the bonding was performed at room temperature. However, due to the long cure times required, elevated temperature curing was used after the first few specimens to shorten the down time between tests. The procedure for bonding the load plates to the specimens is shown in Table 1. A special fixture was made to properly align the load plates and the specimen during bonding to minimize any moments that would be introduced during testing. The fixture with a specimen between the load plates is shown in Figure 5. The fixture, a steel plate with the four pins that penetrate the holes in the load plate tabs, aligns the load plates during bonding so that the shear stress is applied during testing without any undesired moments. After each test was completed, the load plates were removed from the specimen, cleaned, and rebonded to the next specimen.
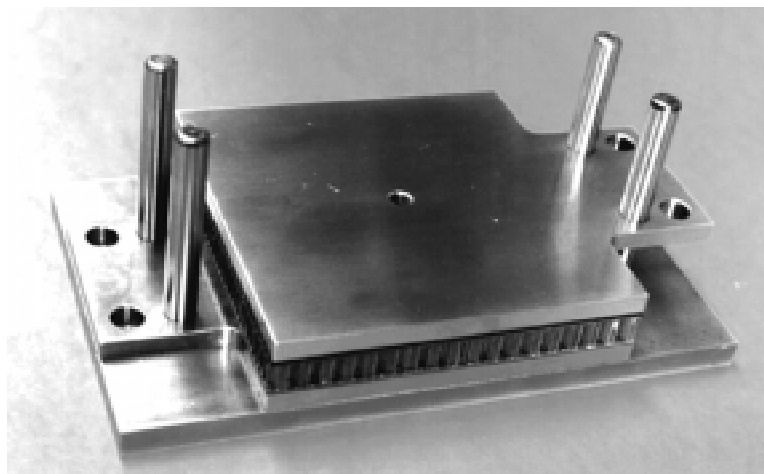

Figure 5:   Photograph of a specimen in the bonding fixture between two load plates.

Table 1: Procedure For Bonding Sandwich Panel Specimens to Load Plates

1. Clean both surfaces of the sandwich core specimen with ethyl alcohol
2. Sandblast sandwich core specimen
   a) Mask the sides of the specimen with tape
   b) Mask the drilled holes with tape
   c) Place the specimen in the sandblasting cabinet
   d) Adjust the compressor pressure to 40 psi
   e) Set the air pressure for blasting at 20 psi by adjusting the regulator attached to the cabinet
   f) Start the reclaimer
   g) Position the workpiece conveniently in the cabinet so that the gun can comfortably scan the entire surface of the specimen from a distance of six inches from the surface of the specimen
   h) Press the foot pedal to operate the gun
   i) Hold the gun about six inches from the face of the specimen and blast the entire surface uniformly
   j) Shut off airflow
   k) Shut off reclaimer
   l) Open window and remove specimen
   m) Ensure both sides of the specimen are properly cleaned
3. Clean both surfaces of the sandwich core specimen with ethyl alcohol
4. Place specimen in clean zip lock bags until bonding
5. Sandblast the load plates
   a) Clean all the surfaces with ethyl alcohol prior to inserting in the sandblaster
   b) Follow the same procedure as used for sandblasting the specimens except use a pressure of 40 psi
   c) Sandblast only the surface to be bonded
   d) Clean all the surfaces with ethyl alcohol after removing from the sandblaster
6. Place the load plates in clean zip lock bags until bonding
7. Prepare adhesive according the manufacturers instructions
8. Place the load plate with the hole for the air supply in the bonding fixture with the 1-in-diameter hole facing up
9. Apply a thin layer of adhesive on the surface of the load plate, carefully avoiding the hole in the center
10. Place the sandwich core specimen on the adhesive coated load plate with the holes facing down
11. Apply a thin layer of adhesive to the surface of the other load plate
12. Place the load plate on top of the specimen in the fixture. Ensure that the tabs on the load plates are in the opposite direction
13. Place a piece of rubber over the top load plate
14. Place 5 psi on top of the rubber sheet and allow to set for 1 hour at 150°F

Discussion of Results

All tests were performed at ambient conditions. Two different honeycomb cores were tested: Hexcel HRP-3/16-8.0 and DuPont Korex-1/8-4.5. The Hexcel HRP-3/16-8.0 has a 3/16 in. cell size and an 8.0 lb/ft^3 density. The DuPont Korex-1/8-4.5 has a 1/8 in. cell size and an 4.5 lb/ft^3 density. Both static and cyclic loads were applied parallel (ribbon direction) and perpendicular (transverse direction) to the core ribbon. Non-reversed and fully reversed cyclic loads were studied. ASTM C 273 states that the load should pass through the edge of the specimen.

Figure 6:   Photograph of specimen in test machine with plum line showing load path through the corner of the specimen as stated in ASTM C 273.

The photograph in Figure 6 shows a specimen in the test machine with a "plumb line" along the load path. As can be seen in the photograph, the plum line passes through the corners of the specimen. Permeability was measured simultaneously with the increasing load (or stress), and reported as measured flow rate divided by the applied pressure.

Static Tests

For the static tests, the specimens were loaded to the ultimate shear strength of the honeycomb cores at a rate of 4500 lb/min, which is recommended by ASTM C 273. Two specimens were used for each material in each orientation. The matrix for the static tests is shown in Table 2, along with the ultimate shear stress.

Table 2: Ultimate Shear Stress Under Static Loads for Honeycomb Sandwich Panels.

Material	Orientation	Specimen No.	Ultimate Shear Stress, psi	Avg.
HRP-3/16-8.0	Ribbon	2	450	449.5
		9	449	
	Transverse	3	361	369.5
		11	378	
Korex-1/8-4.5	Ribbon	5	348	344.5
		8	341	
	Transverse	6	231	228.5
		10	226	

The permeability, which is defined as the measured flow rate divided by the applied pressure, is shown in Figure 7 for each of the HRP and Korex specimens as a function of applied shear stress. The permeability is plotted to only 5 ml/min/psi, though in the case of the HRP core, failure occurred at higher values. Definite trends can be seen from the data. The ribbon direction is the stronger direction, as indicated in Table 2, and resists

9

increases in air flow for higher loads. In addition, the sandwich panels made with the Korex core are not as strong as those made with the HRP core. However, the most interesting aspect of the data is that the Korex core permeability seemed to increase instantaneously when the core failed, with no significant increase prior to failure. The HRP specimens experienced an increase in the permeability prior to failure, and the failure appeared to be a bondline failure.
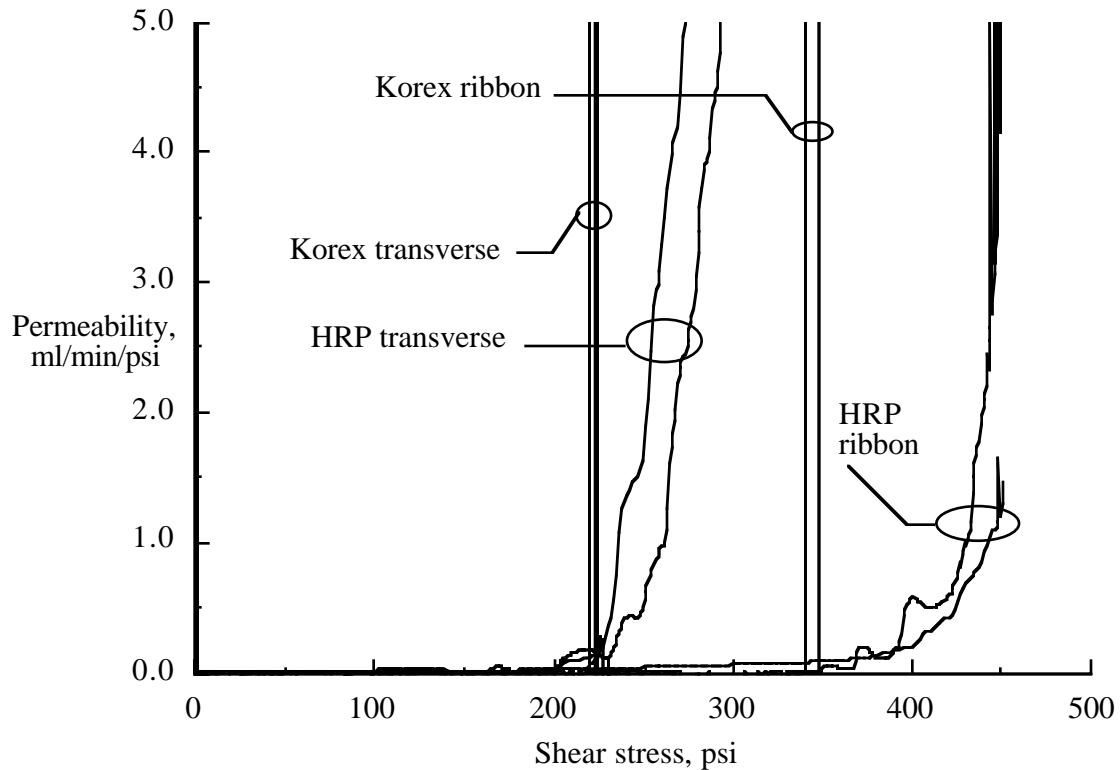

Figure 7: Permeability of HRP and Korex core specimens as a function of applied shear stress.
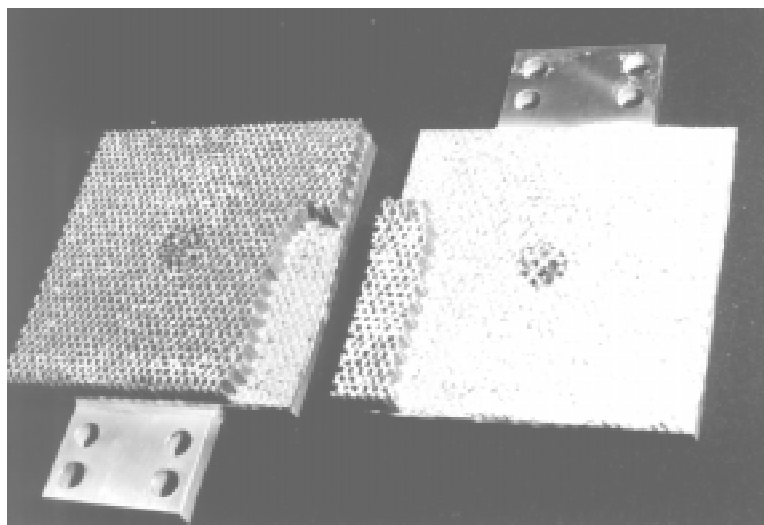

Figure 8: Photograph showing the typical bondline failure mode of the HRP specimens.

Figure 8 shows a photograph of a typical HRP sample after failure. In the figure, it can be seen that the core failed at the bondline. This would seem to indicate that testing of further adhesives may be warranted with the HRP core to increase the failure load by shifting the failure from the bondline to the core.

Dynamic Tests

Air flow measurements were also made at stress amplitudes between the ultimate shear strength, S_{su}, and the endurance limit, S_{se}, of each honeycomb material. Data for a typical S-n plot was generated by subjecting the specimens to a stress level for n_f cycles. Data was obtained for both fully reversed and non-reversed cyclic loads. The permeability was measured at regular intervals as the number of cycles increased. The data sampling rate was decreased as the load was decreased. The maximum number of cycles was approximately 10^6. A loading rate of 5 Hz was used, but was increased to 10 Hz for some of the specimens that were anticipated to run for extended cycles, and was decreased to 2 Hz for specimens that were anticipated to run for only a limited number cycles. Care was taken to obtain a load rate low enough that no significant changes in temperature were present that altered the mechanical properties of the core.

Non-Reversed

The test matrix for the non-reversed fatigue tests is shown in Table 3 along with the specimen number, the shear stress, and the number of cycles to failure. In order to get an idea of how the applied shear stress compared to the ultimate static shear stress given in Table 2, the shear stress is also given in terms of the percentage of the ultimate static shear stress. In specimen number 30, the core failed, which was unusual for the HRP specimens since most failed at the bondline. Specimen number 41 was bonded incorrectly, and as a result, no permeability data was obtained, though failure was determined.

During the tests, air flow measurements were made while the specimens were being subjected to cyclic loads. The cyclic loading was done at different stress amplitude levels for different specimens, ranging from 94% of the ultimate static shear strength downwards. Data sets, acquired at intervals of 1 ms, were stored at pre-determined time intervals. Results from the first two or three tests gave the appropriate trend of the S-n relation, enabling the determination of the amplitude levels for the subsequent tests.

Initial plans called for eight specimens to be tested in the fully reversed mode for each type of panel, and two non-reversed specimens for each type of panel. However, during the initial reversed testing, the fixture connecting the load plates to the load cell broke due to fatigue. A second fixture was then procured from Wyoming Test Fixtures and it again broke. At that point, two fixtures were fabricated locally that were much stronger than the ones used previously. It was then decided to switch the testing and do eight non-reversed and three fully reversed for each type of specimen. The two new fixtures were successfully used for the remainder of the non-reversed tests.

Figure 9 shows the S-n plot for the non-reversed fatigue tests for each of the four different types of specimens. In each case, the data point plotted is for the number of cycles to failure. The average static strength, given in Table 2, is also shown in the figure as the data for 1 cycle. As is consistent with Boeing's prior tests [10], the Korex core failed at lower loads than the HRP core specimen. However, the S-n curve is much flatter for the Korex core specimen than for the HRP core, indicating that Korex failure load is less of a function of the number of cycles than is the HRP failure load. For each

case, the data are fit with a logarithmic curve fit, which appears linear on the semi-log plot.

Table 3: Non-Reversed Fatigue Test Matrix for Honeycomb Sandwich Panels.

Material	Orientation	Spec. No.	Max. shear stress, psi		No. cycles to failure
HRP-3/16-8.0	Ribbon	29	220	(49%)	1001310
		28	264	(59%)	92210
		27	308	(69%)	26520
		26	352	(78%)	5795
		40	375	(83%)	2480
		25	400	(89%)	248
	Transverse	34	185	(50%)	691572
		32	195.5	(53%)	643127
	(core failed)	30	207	(56%)	157465
		31	218.5	(59%)	70703
		33	223.1	(60%)	33500
		37	238	(64%)	28022
		38	248	(67%)	35858
		39	260	(70%)	42925
	(no perm., bonded wrong)	41	300	(81%)	780
		42	320	(87%)	800
Korex-1/8-4.5	Ribbon	18	238	(69%)	1000000
		19	255	(74%)	303985
		16	272	(79%)	42104
		20	289	(84%)	23850
		35	306	(89%)	39927
		15	306	(89%)	23655
		17	323	(94%)	833
	Transverse	22	180	(78%)	699250
		24	186	(81%)	259684
		7	190.9	(84%)	18645
		23	197	(86%)	37482
		36	198	(87%)	990
		21	202.5	(89%)	468

Figure 9 shows the S-n curve for both the HRP and Korex cores for failure. The Korex core experienced negligible increase in permeability until the core failed, at which point the permeability increased significantly. The HRP core, however, experienced a gradual increase in permeability. Figure 10 shows the S-n curve for the HRP core in the ribbon (solid lines) and transverse (dashed lines) directions at different flow rates, i.e., permeability values. Since the Korex core failed catastrophically, an S-n curve for different values of permeability is not of value since all the curves would fall on the same line as the failure S-n curve shown in Figure 9. S-n curves are plotted for the number of cycles it took to initially reach a permeability of 1, 2, and 4 ml/min/psi at the applied test load. The failure S-n cure is also shown on the figure. In the ribbon direction, failure occurred at loads near a permeability of 4 ml/min/psi. However, for the transverse direction, there was a significant increase in the load from 4 ml/min/psi to failure. This

trend, which will be further confirmed in later figures, indicates a more gradual increase in permeability with load for the transverse direction than the ribbon direction.
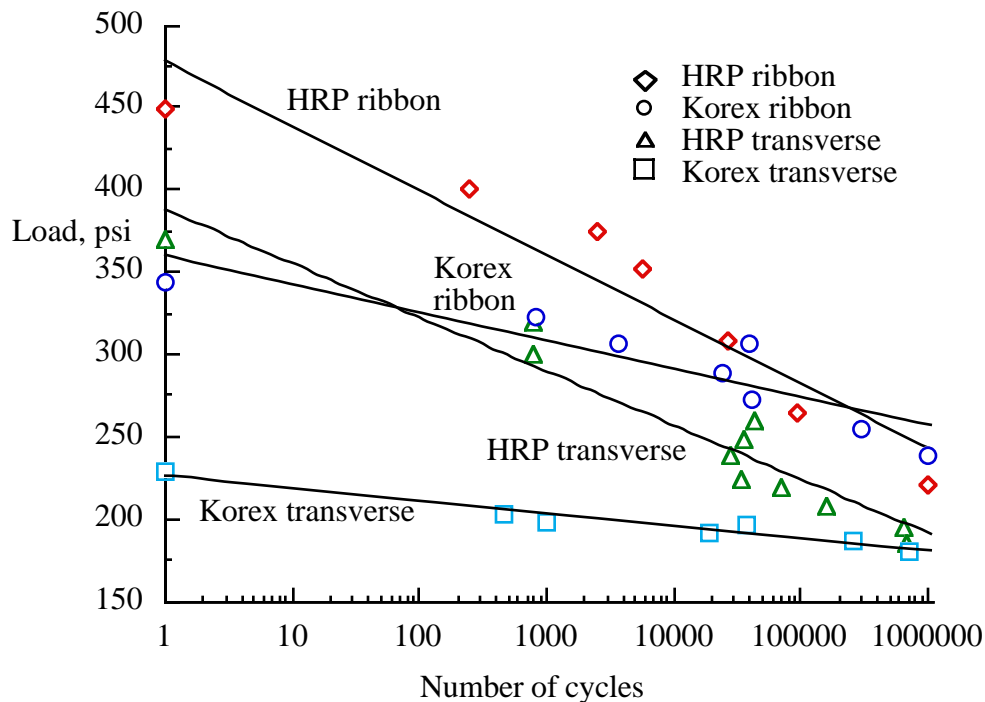

Figure 9: S-n curve for non-reversed fatigue tests of sandwich core panels with number of cycles to failure.
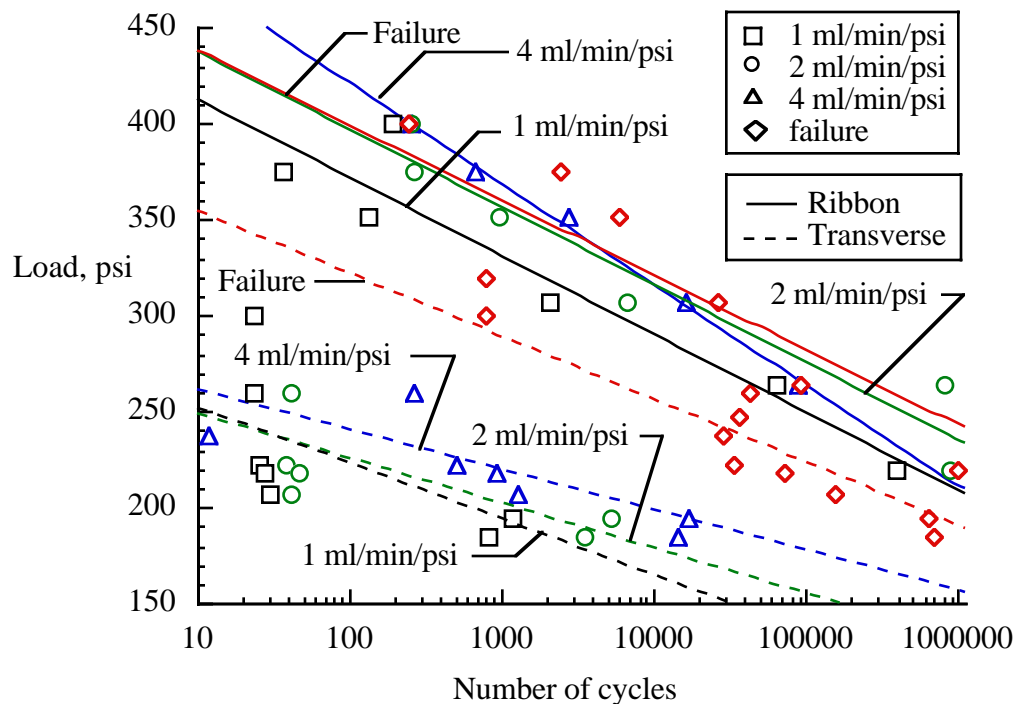

Figure 10: Non-reversed S-n curve showing load versus number of cycles to failure and load versus number of cycles to reach permeability values of 1, 2, and 4 ml/min/psi for the HRP core in both the ribbon and transverse direction.
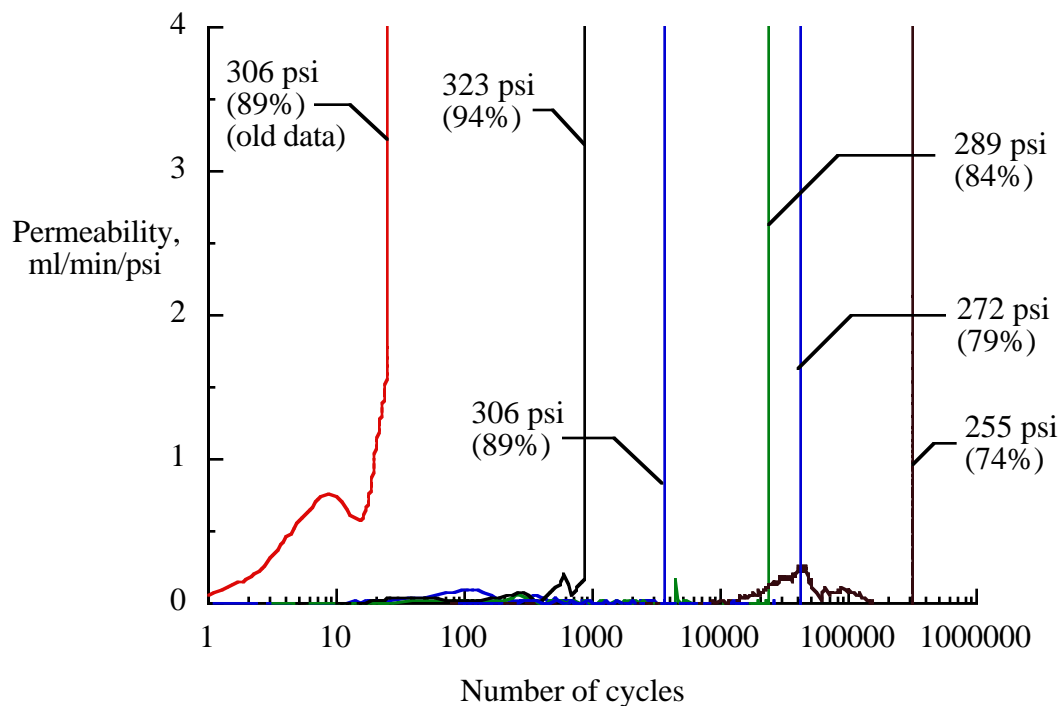
Figure 11:   Permeability as a function of number of cycles for non-reversed fatigue tests with Korex core in the ribbon direction (avg. static shear strength of 344.5 psi).
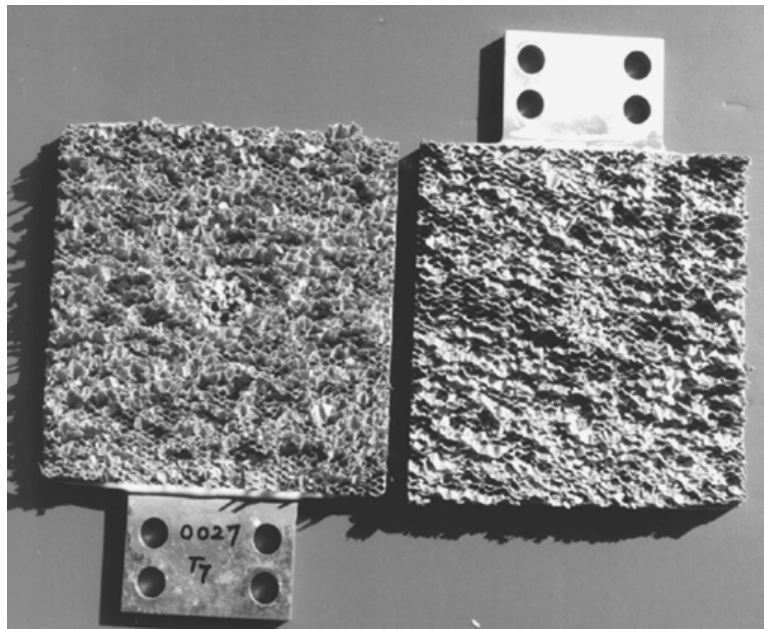
Figure 12:   Photograph of a Korex core specimen after failure.

Figure 11 shows the permeability versus number of cycles for the Korex core in the ribbon direction. Again, the permeability is defined as flowrate divided by stress level. The average static shear strength is 344.5 psi (see Table 2) and the percent of the shear strength is also shown in the figure. The number of cycles to failure, which in the case of

the Korex core corresponds to the sudden increase in permeability, increased with load except for a case with 306 psi. The case with a 306 psi load was rerun and the permeability was in the expected range. Figure 12 shows a photograph of the Korex core after failure. From the photograph, it can be seen that the core failed in the internal portion of the core, and not at the bondline. This is in contrast to the HRP core failure shown in Figure 8 where the failure occurred at the bondline.

Figure 13 shows the permeability versus number of cycles for the Korex core in the transverse direction. As expected, the average static shear strength (228.5 psi) is lower than for the ribbon direction. The permeability again increased almost instantaneously at failure, with negligible air flow prior to failure. Though the number of cycles to failure did not increase with decreased load for all cases, i.e. the 197 psi case, the general trend was that an increased load resulted in a decreased number of cycles to failure.
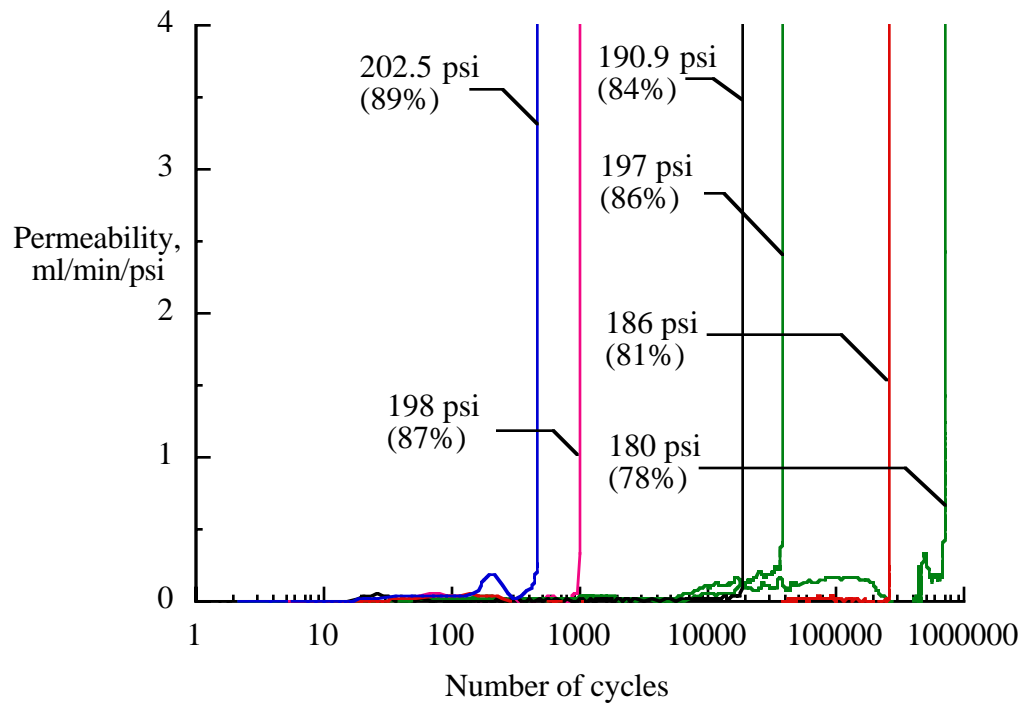

Figure 13: Permeability as a function of number of cycles for non-reversed fatigue tests with Korex core in the transverse direction (avg. static shear strength of 228.5 psi).

Figure 14 shows the permeability versus number of cycles for the HRP core in the ribbon direction. Increased load results in a decreased number of cycles to reach permeability values of 4 ml/min/psi. The major difference between the Korex and HRP core can be seen by comparing the shape of the curves in Figure 14 with those in Figure 11 and Figure 13. In Figure 14, there is a gradual increase in the permeability with an increase in the number of cycles. As mentioned previously, and shown in Figure 8, the HRP samples generally failed at the bondline between the core and the facesheet. The bondline failure appears to be gradual and grows with increased cycles. In contrast, the Korex core samples generally catastrophically failed in the core material, resulting in a sudden increase in the permeability. Several of the HRP samples also experienced an inflection in the permeability as the number of cycles was increasing.
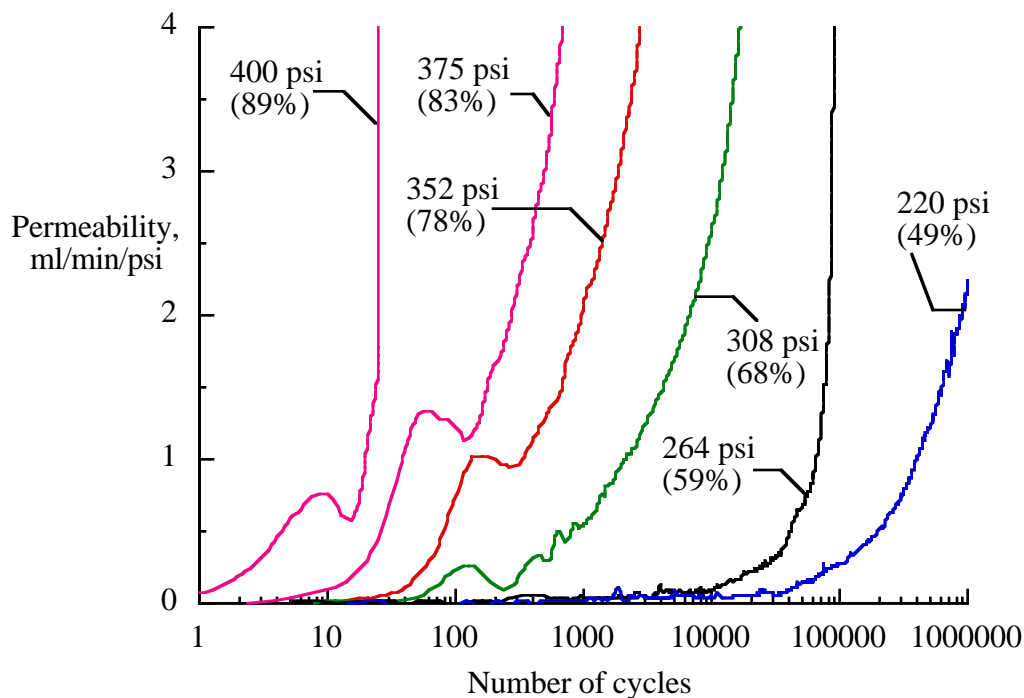
Figure 14: Permeability as a function of number of cycles for non-reversed fatigue tests with HRP core in the ribbon direction (avg. static shear strength of 449.5 psi).
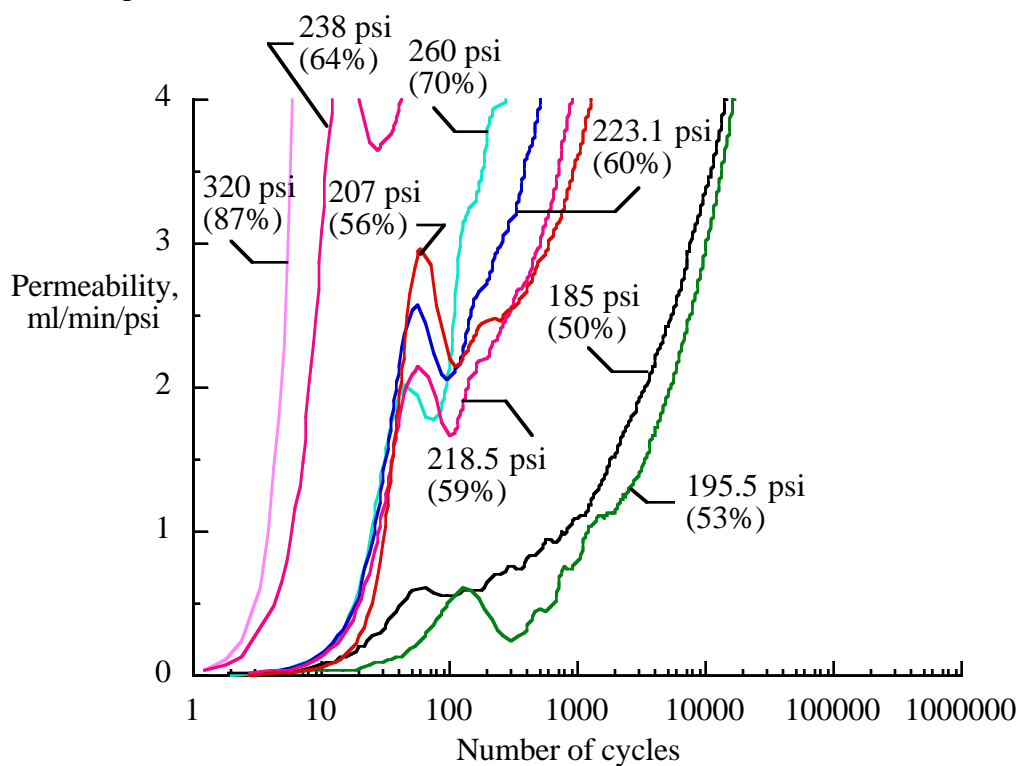

Figure 15: Permeability as a function of number of cycles for non-reversed fatigue tests with HRP core in the transverse direction (avg. static shear strength of 369.5 psi).

Figure 15 shows the permeability versus number of cycles for the HRP core in the transverse direction. The data from test numbers 38 and 41 are not shown in the figure due to bad air flow rate data and improper bonding, respectively. In general, increased load results in a decreased number of cycles to reach permeability values of 4 ml/min/psi. Again, there is a gradual increase in the permeability with an increase in the number of cycles. However, as seen in Figure 10, the increase in permeability with load is more gradual for the transverse direction than the ribbon direction. As with the samples in the ribbon direction, several of the transverse HRP samples also experienced an inflection in permeability as it was increasing. The inflection appears to be larger for the transverse specimens than the ribbon specimens. In this figure, the inflection occurs at higher permeability values for higher loads. From this figure, it would appear that the inflection in the permeability is physical, and is not due to noise in the data acquisition system. Also leading to the thought that the inflection is physical and not noise in the data acquisition is the fact that the permeability experiences both a translation and a change in its rate of increase after the inflection. However, the physical reason for the inflections is not apparent.

Reversed

For the reversed tests, fewer specimens were tested for each orientation. As a result of the reduced specimen number, fewer data points were available to generate the S-n curve. The matrix for the reversed fatigue tests is shown in Table 4 along with the shear stress level and the number of cycles to failure. In order to get an idea of how the applied shear stress compared to the ultimate static shear stress given in Table 2, the shear stress is also given in terms of the percentage of the ultimate static shear stress. As can be seen from the data in Table 4, the number of cycles to failure is significantly less when the load is reversed than when the applied load is non-reversed (see Table 3).

Table 4: Fully Reversed Fatigue Test Matrix for Honeycomb Sandwich Panels.

Material	Orientation	Spec. No.	Shear stress, psi		No. cycles to failure
HRP-3/16-8.0	Ribbon	54	± 240	(54%)	41,494
		52	± 272	(61%)	15,761
		53	± 305	(68%)	1899
	Transverse	51	± 120	(32%)	552,307
		50	± 160	(43%)	7541
		49	± 200	(54%)	1914
		48	± 290	(78%)	30
Korex-1/8-4.5	Ribbon	45	± 204	(59%)	117,955
		44	± 238	(69%)	13,313
		43	± 272	(79%)	1560
	Transverse	55	± 170	(74%)	1,601
		47	± 183	(80%)	759
		46	± 189	(83%)	76

Figure 16 shows the S-n curve for the Korex and HRP core specimens for failure. As with the non-reversed tests, the Korex core curve in the transverse direction is relatively flat, indicating that the transverse direction failure is very sensitive to load, i.e., a small increase in the transverse direction load results in a significant decrease in the number of cycles to failure. However, the Korex core in the ribbon direction is not as flat as it was in the non-reversed case, and in fact is similar in slope to the HRP transverse core. As in the non-reversed case, the Korex core in the ribbon direction is stronger than

the HRP core in the transverse direction, but the differences are greater for the fully reversed than the non-reversed.

As with the non-reversed tests, the Korex specimens experienced little increase in permeability prior to catastrophic failure. However, specimen number 47 did survive approximately 50 cycles as the permeability increased from 0.1 ml/min/psi to 0.4 ml/min/psi. Though this permeability value and the number of cycles are very small relative to the HRP core specimens, they are unusual for the Korex core specimens.
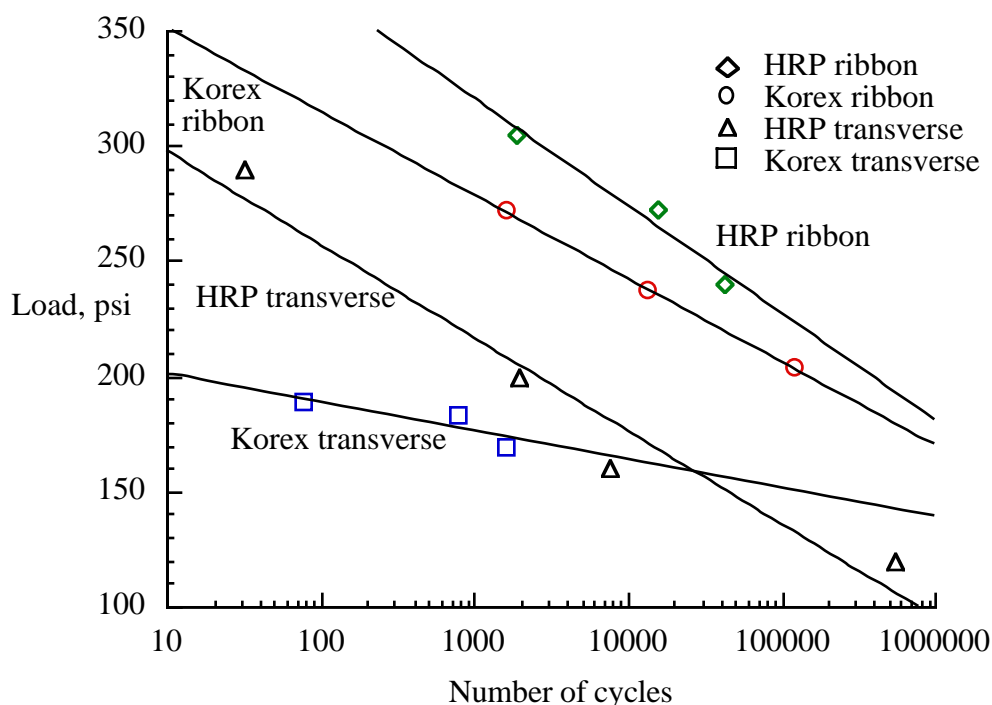
Figure 16: S-n curve for fully reversed fatigue tests of sandwich core panels with number of cycles to failure.

Figure 17 shows the S-n curve for the HRP core in both the ribbon and transverse directions. The figure shows the load versus number of cycles to failure and load versus number of cycles to reach permeability values of 1, 2, and 4 ml/min/psi for each core. The data points in the figure are for the number of cycles the specific permeability value is reached. The ribbon curves are shown with the solid line and the transverse curves with the dashed line. The curves for the ribbon direction are steeper than those for the transverse direction.

Figure 18 shows the permeability as a function of number of cycles for fully reversed fatigue tests with HRP core in the transverse direction. The percentage of the shear strength is also shown on the figure. As mentioned previously, the permeability increases much more rapidly (implying core degradation) for the fully reversed loading than the non-reversed loading. An inflection in the permeability is noticed in the 160 psi and 200 psi cases, but not in the 120 psi or 290 psi cases. As mentioned earlier, the cause of the inflection is unknown.
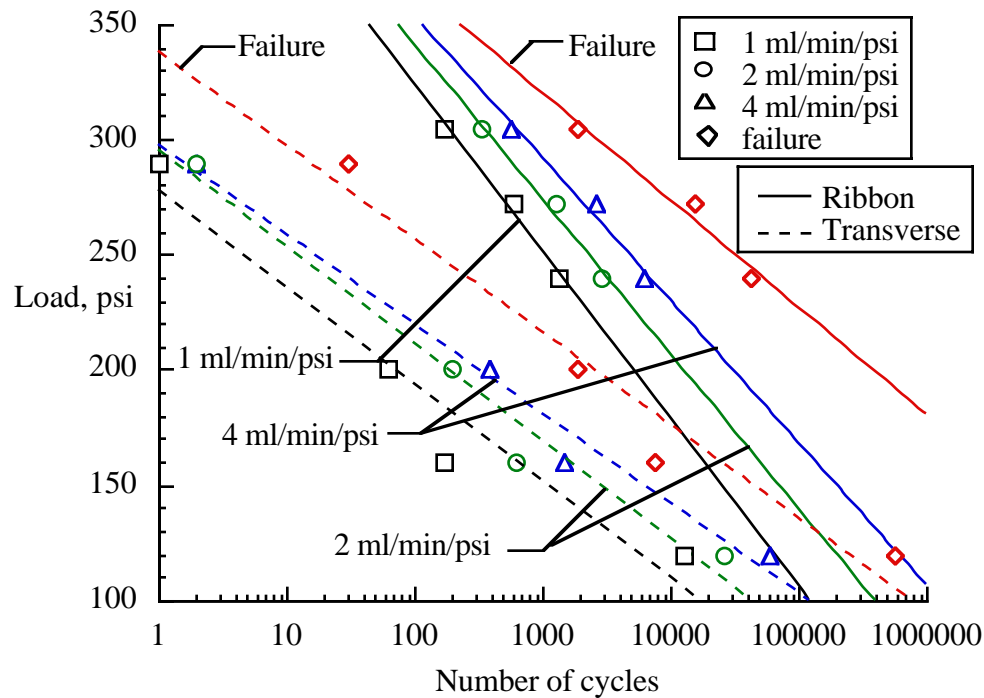
Figure 17:   Fully reversed S-n curve showing load versus number of cycles to failure and load versus number of cycles to reach permeability values of 1, 2, and 4 ml/min/psi for the HRP core in both the ribbon and transverse direction.
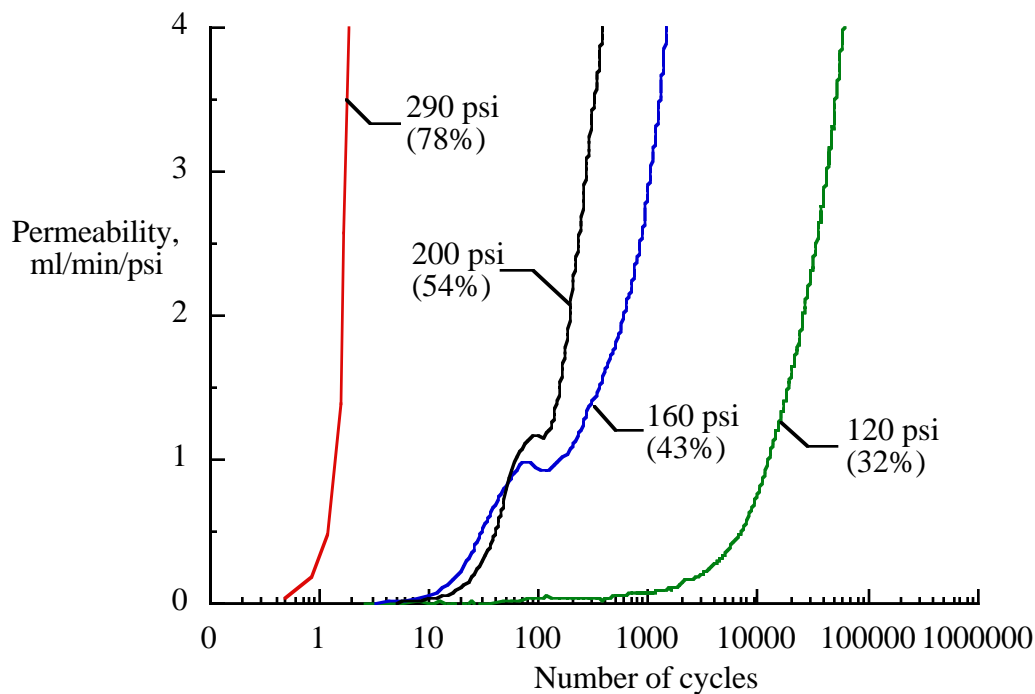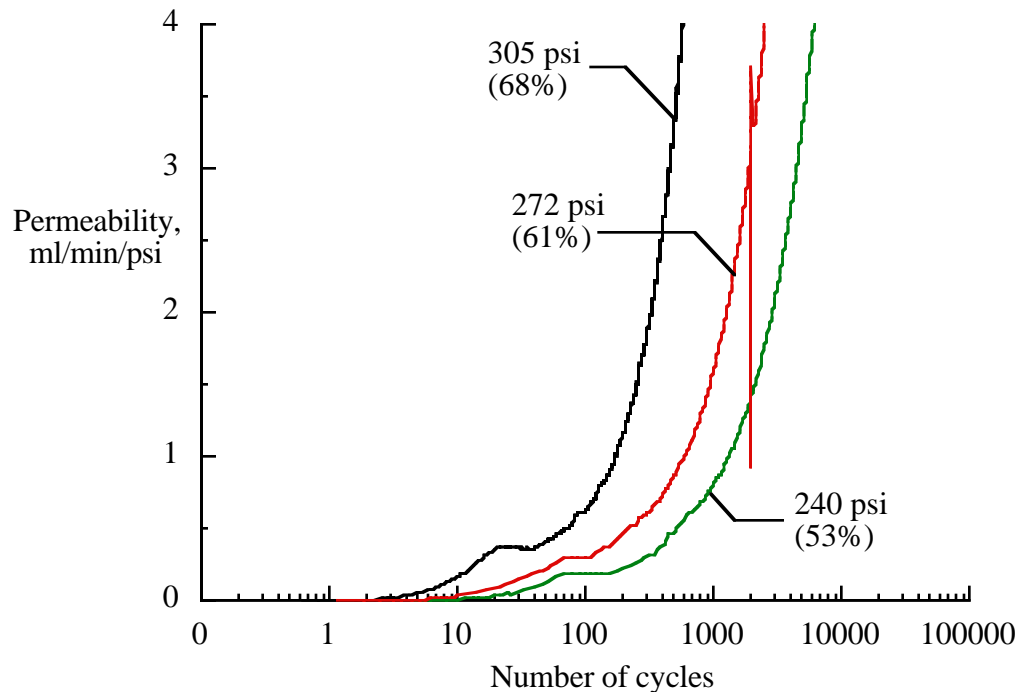

Figure 18:   Permeability as a function of number of cycles for fully reversed fatigue tests with HRP core in the transverse direction (avg. static shear strength of 369.5 psi).

Figure 19 shows the permeability as a function of number of cycles for fully reversed fatigue tests with HRP core in the ribbon direction. Only three specimens were tested with this orientation, and unfortunately, the decrease in load between tests was not enough to spread the data out as much as would have been desired. The 272 psi case experienced a sharp dip in the permeability value near 2000 cycles. It is thought that this dip is noise in the data acquisition system. Some inflection points are also seen in the data.

Figure 19:   Permeability as a function of number of cycles for fully reversed fatigue tests with HRP core in the ribbon direction (avg. static shear strength of 449.5 psi).

Concluding Remarks

Both Hexcel HRP-3/16-8.0 and DuPont Korex-1/8-4.5 honeycomb core sandwich specimens were tested under shear loads. The permeability of the core was measured while the load was applied both statically and dynamically (reversed and non-reversed). The Korex core specimens failed in the honeycomb core, and the permeability increased almost instantaneously at failure. In general, the HRP core failed at the bondline, and the permeability gradually increased until failure. An inflection point was also observed in the permeability of many of the specimens when subjected to cyclic loads. The cause of this inflection point is uncertain. Finally, after several test fixture failures during the fully reversed tests, a test fixture was designed that allowed the fully reversed tests to be performed.

Acknowledgments

References

1. Mabson, G. E.; et al.: "COSTADE for Full-Scale Fuselage," 11th DoD/NASA/FAA Conference on Fibrous Composites in Structural Design, August 1996.

2. Ilcewicz, L. B.; et al.: "Advanced Technology Composite Fuselage - Program Overview," NASA CR-4734, 1997.

3. Komorowski, J. P.: "Hygrothermal Effects in Continuous Fibre Reinforced Composites Part 1: Thermal and Moisture Diffusion in Composite Materials," Aeronautical Note NAE-AN-4, NRC No. 20974, National Research Council Canada, January 1983.

4. Mijovic, J. and Weinstein, S. A.: "Moisture Diffusion in Graphite/Epoxy Composites," Polymer Communications, Vol. 47, 1993.

5. Lee, M. C. and Peppas, N. A.: "Water Transport in Graphite/Epoxy Composites," Journal of Applied Polymer Science, Vol. 47, 1993.

6. Clark, G.: et al.: "Moisture Absorption in Graphite/Epoxy Laminates," Composites Science and Technology, Vol. 39, 1990.

7. Coggeshall, R. L.: "Boeing/NASA Composite Components Flight Service Evaluation," NASA CR 181898, November 1989.

8. Jacobs, P.; and Jones, F.: "Diffusion of Moisture into Two-Phase Polymers, Part 1 The Development of an Analytical Model and Its Application to Styrene-Ethylene/Butylene-Styrene Block Copolymer," Journal of Materials Science, 1989.

9. D. B. Scholz, L. B. Ilcewicz, R. J. Karch, R. S. Lakes, D. M. Cise, D. E. Glass, and V. V. Raman, "Environmental Durability of Composite Fuselage Sandwich Structure", 11th DoD/NASA/FAA Conference on Fibrous Composites in Structural Design, Fort Worth, TX, August 26-29, 1996.

REPORT DOCUMENTATION PAGE

1. AGENCY USE ONLY (Leave blank)	2. REPORT DATE	3. REPORT TYPE AND DATES COVERED
	December 1997	Contractor Report

4. TITLE AND SUBTITLE

Honeycomb Core Permeability Under Mechanical Loads

6. AUTHOR(S)

David E. Glass, V. V. Raman, Venki S. Venkat, and Sankara N. Sankaran

5. FUNDING NUMBERS

NAS1-20013

WU 538-13-11-02

7. PERFORMING ORGANIZATION NAME(S) AND ADDRESS(ES)

Analytical Services & Materials, Inc.
107 Research Drive
Hampton, VA 23669-1340

8. PERFORMING ORGANIZATION REPORT NUMBER

AS&M-R53-97-01

9. SPONSORING/MONITORING AGENCY NAME(S) AND ADDRESS(ES)

National Aeronautics and Space Administration
NASA Langley Research Center
Hampton, VA 23681-2199

10. SPONSORING/MONITORING AGENCY REPORT NUMBER

NASA/CR-97-206263

11. SUPPLEMENTARY NOTES

This report was prepared for Langley under contract NAS1-20013, by The Boeing Company, Seattle, WA, under subcontract to Analytical Services & Materials, Inc., Hampton, VA.
Langley Technical Monitor: William D. Brewer

12a. DISTRIBUTION/AVAILABILITY STATEMENT

Unclassified-Unlimited
Subject Category 24   Distribution: Standard
Availability: NASA CASI (301) 621-0390

12b. DISTRIBUTION CODE

13. ABSTRACT (Maximum 200 words)

A method for characterizing the air permeability of sandwich core materials as a function of applied shear stress was developed. The core material for the test specimens was either Hexcel HRP-3/16-8.0 and or DuPont Korex-1/8-4.5 and was nominally one-half inch thick and six inches square. The facesheets where made of Hercules' AS4/8552 graphite/epoxy (Gr/Ep) composites and were nominally 0.059-in. thick. Cytec's Metalbond 1515-3M epoxy film adhesive was used for co-curing the facesheets to the core. The permeability of the specimens during both static (tension) and dynamic (reversed and non-reversed) shear loads were measured. The permeability was measured as the rate of air flow through the core from a circular 1-in2 area of the core exposed to an air pressure of 10.0 psig. In both the static and dynamic testing, the Korex core experienced sudden increases in core permeability corresponding to a core catastrophic failure, while the HRP core experienced a gradual increase in the permeability prior to core failure. The Korex core failed at lower loads than the HRP core both in the transverse and ribbon directions.

14. SUBJECT TERMS

Honeycomb, mechanical properties, permeability

15. NUMBER OF PAGES

25

16. PRICE CODE

A03

17. SECURITY CLASSIFICATION OF REPORT	18. SECURITY CLASSIFICATION OF THIS PAGE	19. SECURITY CLASSIFICATION OF ABSTRACT	20. LIMITATION OF ABSTRACT
Unclassified	Unclassified	Unclassified	